Separation Science and Technology
Publication details, including instructions for authors and subscription information:
http://www.informaworld.com/smpp/title~content=t713708471

Copper ion removal by almond shell carbons and commercial carbons: batch and column studies

Christopher A. Toles[a]; Wayne E. Marshall[b]
[a] Cabot Corporation Billerica, MA, U.S.A. [b] Southern Regional Research Center, New Orleans, LA, U.S.A.

To cite this Article Toles, Christopher A. and Marshall, Wayne E.(2002) 'Copper ion removal by almond shell carbons and commercial carbons: batch and column studies', Separation Science and Technology, 37: 10, 2369 — 2383

To link to this Article: DOI: 10.1081/SS-120003518

URL: http://dx.doi.org/10.1081/SS-120003518

SEPARATION SCIENCE AND TECHNOLOGY, 37(10), 2369–2383 (2002)

COPPER ION REMOVAL BY ALMOND SHELL CARBONS AND COMMERCIAL CARBONS: BATCH AND COLUMN STUDIES

Christopher A. Toles[1] and Wayne E. Marshall[2,*]

[1]Cabot Corporation Billerica, MA 08121
[2]USDA-ARS, Southern Regional Research Center,
New Orleans, LA 70179, USA

ABSTRACT

Phosphoric acid-activated/oxidized, and steam-activated and steam-activated/oxidized almond shell granular activated carbons (GACs) were investigated for their utility in removing copper ion (Cu^{2+}) from solution in both batch and column applications compared to commercially available GACs. Adsorption isotherms were developed and found to best fit the Freundlich model. Experimental and commercial carbons were packed into columns and exposed to two different empty bed contact times using a solution of 3 m*M* $CuCl_2$ buffered at pH 4.8. The most effective GACs for removal of copper ions in batch mode were the phosphoric acid-activated/oxidized and steam-activated/oxidized experimental carbons. The most effective carbon in column mode appeared to be the phosphoric acid-activated/oxidized sample. A column packed with this carbon showed higher breakthrough volumes and greater estimated hours of operation than other

---

[*] Corresponding author.

experimental carbons and commercial carbons evaluated. This carbon could function as an effective metal ion adsorbent in water and wastewater treatment.

INTRODUCTION

As clean water concerns increase, a variety of remediation methods are being developed. Organic contaminants in water are not the only concern. Metals in the form of metal ions ubiquitously pervade both surface and groundwater sources. Removal normally consists of precipitation with an inexpensive base, such as calcium or sodium hydroxide, which can be followed by treatment with a cation exchange resin. Activated carbons are usually associated with removal of organic contaminants, especially those contaminants that impart taste and odor to potable water. However, they have also been shown to have some effect on the removal of metal ions from solution under both batch and column conditions (1–5).

Our laboratory at the Southern Regional Research Center has developed GACs from various tree nut shells that are particularly effective in metal ion adsorption (6–8). The tree nutshells were chemically activated with phosphoric acid and concurrently oxidized with air during activation. One particular nutshell investigated as a carbon feedstock was almond shell. The U.S. almond shellers produced 376,400 metric tons of shelled almonds in 1999 (9). This resulted in 309,000 metric tons of shell. While the entire U.S. carbon demand cannot be met using only almond shells as feedstock, establishing a niche market for effective metal ion-adsorbing carbons is possible.

Our laboratory has shown that phosphoric acid-activated almond shells may provide an effective GAC for both metal ion and organics adsorption (7,8). These carbons show excellent adsorption of copper ion (7) and good adsorption of a mixture of polar and nonpolar low molecular weight organic compounds (8) in batch adsorption studies.

Measuring adsorption properties of GACs in batch mode determines important equilibrium parameters such as adsorption capacity and adsorption efficiency at a given adsorbate concentration. However, GAC adsorption characteristics should also be investigated in column mode to effectively model nonequilibrium adsorption under industrial separation conditions. In column studies, the solution may only be in contact with the entire length of the adsorbent bed for a matter of minutes. In this case, adsorption kinetics becomes particularly important. Fast kinetics are desirable where it may not be possible to extend the contact time between the carbon and the adsorbate.

The objective of this study focuses on the metal ion adsorption capabilities of phosphoric acid-activated/oxidized, and steam-activated and steam-activated/

oxidized GACs from almond shells and compares them to the metal ion-adsorption capabilities of select commercial GACs under both batch and column conditions.

EXPERIMENTAL

Materials

Almond shells were obtained from California Almond Hulls, Turlock, CA. The shells were hand separated from the hulls and the shells milled in a Retsch SK100 cross-beater mill (Glen Mills, Clifton, NJ). The shells were sieved to a 10 × 20 mesh (2.00–0.85 mm) particle size before activation.

Three commercial reference carbons, Norit RO 3515 and Norit C (Norit Americas, Atlanta, GA) and Nuchar WV-B (Westvaco, North Charleston, SC) were chosen for comparison. Norit RO 3515 is marketed as a precious metal recovery carbon and is made by steam activation of extruded peat. Norit C is used for removal of organic compounds, such as organic acids, from aqueous media. It is produced by phosphoric acid (H_3PO_4) activation of wood. Nuchar WV-B (14 × 35 mesh) is a versatile carbon used for a variety of liquid and gas applications and is developed from wood by phosphoric acid activation.

Methods

The experimental carbon, AAS71, was produced by mixing almond shells in a 1:1 wt ratio with 50% H_3PO_4 and soaking the mixture for 24 hr. The mixture was placed in a box furnace with retort (Lindberg, Watertown, WI) and the "air-activation" method described by Toles et al. (6) was used. The chemically activated carbon was washed extensively in a Soxhlet apparatus with hot (95–100°C) water for about 20 hr to remove excess phosphoric acid. Both Norit C and Nuchar WV-B, as supplied, were found to contain phosphoric acid from the activation process and were washed in a similar manner to remove phosphoric acid. The absence of phosphate was noted by the absence of a lead phosphate precipitate when several drops of $Pb(NO_3)_2$ were added to the wash water from the Soxhlet extractor. A yield of 42% of the original mass of shells was recorded for AAS71.

The experimental carbon, AS70, was pyrolyzed and steam activated as described by Toles et al. (10). Pyrolysis consisted of heating almond shells to 800°C for 1 hr under a flow of nitrogen gas. After pyrolysis, the retort temperature was kept at 800°C and distilled water was pumped into a stream of nitrogen entering the furnace at a rate of 7 mL/min for 2 hr in order to create steam for activation. After activation, the sample was allowed to cool to room temperature with nitrogen flowing in the retort. The mass yield was 11%.

A portion of the AS70 sample was placed in the furnace and heated to 300°C under flowing nitrogen. When the temperature reached 300°C, nitrogen flow was stopped and breathing grade air was allowed to flow into the retort at a rate of 0.1 m^3/hr for 4 hr in order to oxidize the carbon. After 4 hr, air flow was stopped and the sample was cooled to room temperature under nitrogen. This sample was designated "AAS70." A yield of 9% of the original shell mass was observed.

The BET surface areas were determined on the carbons as described by Toles et al. (6).

Determination of titratable functional groups and acidic surface charge was based on a titrimetric method of Boehm (11) that was modified by Toles et al. (12) using the strong base sodium ethoxide ($NaOC_2H_5$) or sodium hydroxide (NaOH) as titrants, respectively.

The pH values of the carbons were determined by placing 1 g of carbon in 100 mL distilled water, stirring the mixture and measuring pH with an Orion model 710A meter (Orion Research, Inc., Beverly, MA).

Copper ion adsorption isotherms were developed from copper chloride solutions that ranged in concentration from 0.5 to 30 m*M* in 0.07 *M* sodium acetate–0.03 *M* acetic acid buffer, pH 4.8. One gram of carbon was stirred in 100 mL of copper chloride solution at 300 rpm for 24 hr to ensure that equilibrium had been reached. Total and free Cu^{2+} concentrations were obtained from the copper ion assay of Toles et al. (6). The amount of Cu^{2+} bound plus the free Cu^{2+} concentration were used to construct adsorption isotherms. The isotherms were fitted to both the Freundlich and Langmuir adsorption models using the following linear equations:

$$\text{Freundlich}: \log q_e = \log K_f + 1/n \log c_e$$

$$\text{Langmuir}: q_e = -K_a(q_e/c_e) + Q$$

where $q_e =$ amount of Cu^{2+} adsorbed at equilibrium per gram of carbon; $c_e = Cu^{2+}$ concentration at equilibrium; $K_f =$ Freundlich or specific capacity constant; $n =$ measure of energy of the adsorption reaction; $K_a =$ Langmuir or affinity constant; and $Q =$ adsorption capacity.

Linear regression analysis was applied to each set of data points and a correlation coefficient (r^2) and a probability value (p) representing the "goodness of fit" of the Freundlich or Langmuir model to the data was obtained by the linear regression program in SigmaPlot v. 5.0 for Windows 95 (SPSS Inc., Chicago, IL).

Carbon columns were prepared by tamping dry carbon into a 1.6 × 30 cm glass column (Pharmacia, Uppsala, Sweden) with a bed volume of 50 mL. The tamp method of loading the column was sufficiently reproducible as carbon volume differed from column to column by less than 6%. The carbon load was weighed and recorded. Columns were attached to a Manostat "Vera" peristaltic pump (Barnart Co., Barrington, IL) fitted with silicone tubing (ID = 0.16 cm, OD = 0.48 cm).

The influent through the column consisted of a 3 m*M* solution of copper chloride in 0.07 *M* sodium acetate–0.03 *M* acetic acid buffer, pH 4.8. Earlier studies (13) had found that optimum copper ion adsorption for several commercial activated carbons occurred above pH 4. Above pH 6.5, copper ion may precipitate out of solution and foul the column. For this reason, the influent solution was buffered (7). The effluent solution leaving the column was about pH 5.0.

Two influent flow rates of 2 and 10 mL/min were used which yielded Empty Bed Contact Times (EBCT) of 25 and 5 min, respectively, where EBCT = (column bed volume/flow rate).

Adsorption characteristics of the column were presented by measuring the ratio of copper ion concentration at a specific bed volume (C_e) to the copper ion concentration of the influent stream (C_o) or C_e/C_o. This ratio was plotted as a function of the number of bed volumes of effluent passed through the column at a given EBCT.

Breakthrough curves were determined for each of the column experiments. The breakthrough volume (V_b) is often determined by regulatory concerns and is based on a chosen value percentage of the influent metal ion concentration (14,15). In this study, however, we chose the breakthrough volume based on actual experimental data, which we feel, more realistically depicted actual breakthrough of copper ions. V_b was calculated by choosing the last point at or nearest to zero copper ion concentration, as determined by ICP analysis, and the next point on the curve with a greater copper ion value. A line was drawn between these points, and where the line intersected the *x*-axis, this value was designated V_b.

In addition to breakthrough volume, carbon usage rate (CUR) was determined where CUR = [(mass of carbon in column)/V_b] and estimated hours of column operation (EHO) which is also called "time in service to exhaustion" is defined as EHO = [total weight of adsorbent × (adsorbent capacity for adsorbate/hourly load of adsorbate)] (16).

RESULTS AND DISCUSSION

Carbon Properties

Table 1 presents data on selected physical and chemical properties of the carbons used in this study. Commercial carbons were selected for the lignocellulosic nature of the precursor material (peat, wood) and their method of activation (steam, phosphoric acid), both of which represented a reasonable

Table 1. Select Physical and Chemical Properties of Almond Shell-Based Carbons and Commercial Carbons

Sample ID	Activation Method	S_{BET} (m^2/g)	Titratable Groups (mmol H^+ eq/g)	pH
Almond shell GACs				
AAS71	H_3PO_4 + air	1395	1.73[a]/(1.32[b])	3.59
AS70	Steam	436	1.12/(−0.40)	10.4
AAS70	Steam + air	497	1.76/(−0.41)	10.45
Commercial GACs				
Norit RO 3515	Steam	857	0.28/(−0.37)	10.14
Norit C	H_3PO_4	1289	3.05/(1.22)	3.71
Nuchar WV-B	H_3PO_4	1668	2.48/(0.52)	6.65

All values are means of duplicate determinations where the standard error was $<5\%$.

[a] Top values are titratable functional groups measured by sodium ethoxide ($NaOC_2H_5$) titration.

[b] Bottom values in parenthesis are acidic surface charge measured by sodium hydroxide (NaOH) titration.

match for the lignocellulosic almond shell and activation methods used to produce almond shell carbons. All three acid-activated carbons (AAS71, Norit C, Nuchar WV-B), including the two commercial carbons, had surface areas greater than 1000 m^2/g. In contrast, the steam activated carbons (AS70, AAS70, Norit RO 3515) had surface areas below 900 m^2/g, with surface areas below 500 m^2/g for the almond shell carbons.

Acid-activated carbons generally exhibited higher values for titratable functional groups than the steam-activated carbons. Acid-activated carbons had acidic surfaces as evidenced by their net negative surface charge. Net negative surface charge was related to carbon pH as the acid-activated carbons were acidic. Steam activated carbons had net positive surface charge and basic pH values. The method of activation was more influential in determining the number and kinds of titratable surface groups and pH than the carbon precursor (almond shells, wood, or peat).

Adsorption Isotherms—Batch Experiments

Figure 1 shows the adsorption isotherms for the phosphoric acid-activated carbons. None of the carbons appears to display saturation behavior, even at high copper ion concentrations. All three carbons appear to become saturated at equilibrium metal ion concentrations of 15 m*M* and below. However, at higher

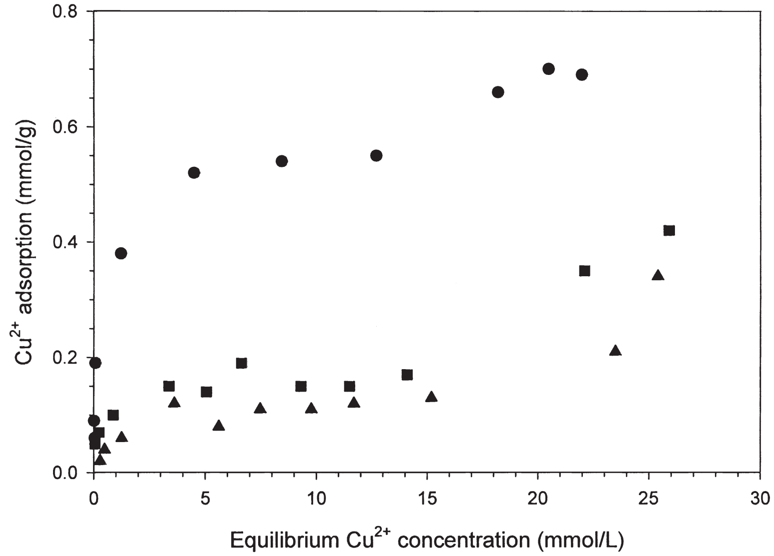

Figure 1. Adsorption isotherms for phosphoric acid-activated, almond shell-based carbon, AAS71 (●), and phosphoric acid-activated, wood-based commercial carbons, Norit C (■), and Nuchar WV-B (▲).

equilibrium copper ion levels, the carbons adsorb additional metal ion. This may be due to the development of a second layer of metal ion coverage on the adsorbing surfaces of the carbons (17). In any case, the acid-activated almond shell carbon (AAS71) adsorbed more copper ion than either wood-based commercial carbon at all copper ion concentrations. During acid activation of the almond shells, a combination activation/oxidation treatment was applied. As far as we know, only an activation treatment in the presence of an inert gas was carried out to produce the two commercial carbons. Therefore, oxidative treatment of almond shells using air may have resulted in the high negative surface charge observed in Table 1 and greater copper ion adsorption.

Figure 2 depicts adsorption isotherms for the steam-activated carbons. For these carbons, saturation of the copper ion adsorption sites was not achieved, even at equilibrium metal ion concentrations over 20 m*M*. The steam-activated, oxidized almond shell carbon adsorbed more copper ion under these conditions than the carbons that were only steam activated and not oxidized. As appears to be the case with acid-activated carbons, an oxidative treatment appears to have a beneficial effect on metal ion adsorption.

In order to characterize metal ion adsorption, either the Langmuir or Freundlich adsorption models are normally applied to adsorption systems such as

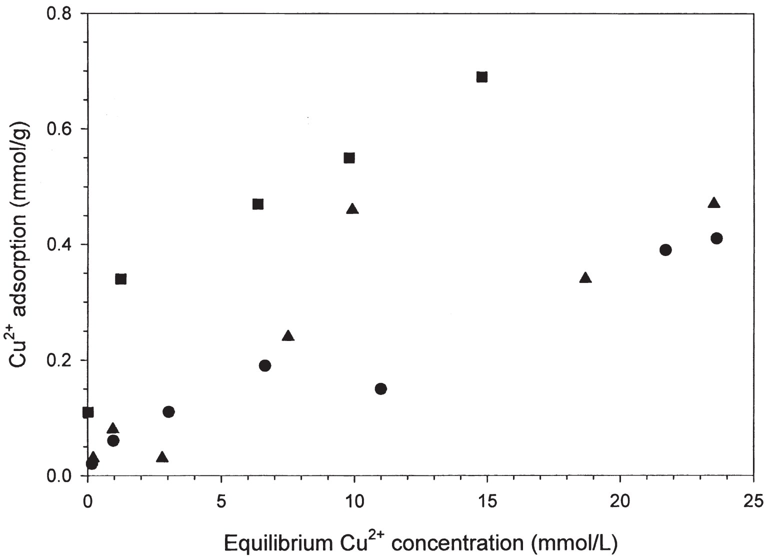

Figure 2. Adsorption isotherms for steam-activated, AS70 (●), and steam-activated/oxidized, AAS70 (■), almond shell-based carbons and a steam-activated, peat-based commercial carbon, Norit RO 3515(▲).

described in Figs. 1 and 2. Since the Langmuir model represents the formation of a monomolecular layer on the surface of the adsorbent, this model would not be applicable to explain the isotherms in Fig. 1. Since surface coverage does not appear to be complete (lack of surface saturation) for the carbons in Fig. 2, the Langmuir model may not be the best choice because it is normally used to describe systems in which adsorption site saturation occurs. When the Langmuir model was applied to the data in Fig. 2, the adsorption constants, K_a and Q, generally had "p" values >0.05, which meant their significance was in doubt (data not shown). In contrast, the Freundlich model describes low and intermediate surface coverage of the adsorbent and is more forgiving than the Langmuir model in describing the exact nature of the coverage, be it monolayer or multilayer. Therefore, we applied the Freundlich model to the isotherms in Figs. 1 and 2 and obtained the linear representations shown in Figs. 3 and 4.

Freundlich constants were obtained from these lines and the values are given in Table 2. The acid-activated carbons all had "n" values of approximately 2 or greater. Steam-activated carbons, especially those without additional oxidation, had "n" values less than 2. If $n > 1$, then the bond energies decrease with surface density. The closer that "n" gets to 1, the more equivalent are the surface sites. K_f, an estimation of bond strength, is highest for the air oxidized

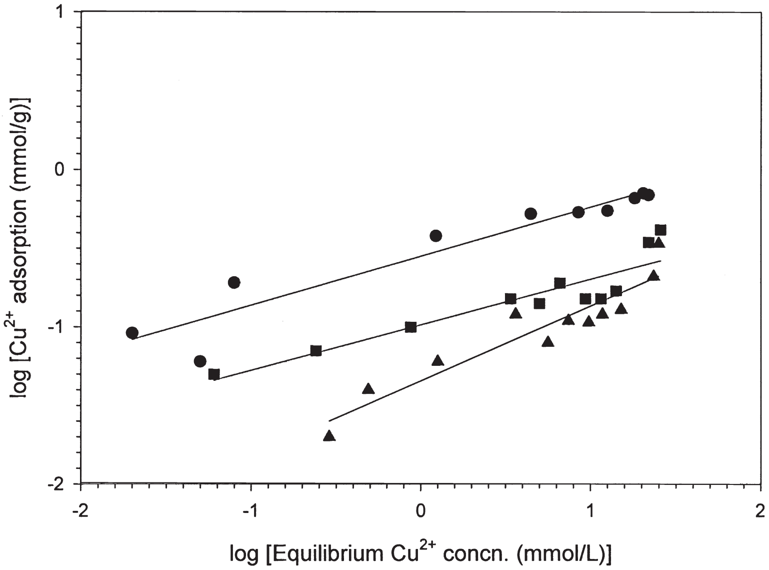

Figure 3. Freundlich plots for phosphoric acid-activated, almond shell-base carbon, AAS71 (●) $r^2 = 0.91$, and phosphoric acid-activated, wood-based commercial carbons, Norit C (■) $r^2 = 0.84$, and Nuchar WV-B (▲) $r^2 = 0.88$.

carbons (AAS70, AAS71) regardless of activation method. These carbons possess the highest adsorption of copper ion (Figs. 1 and 2), which is perhaps due to the relatively stronger surface bond strength between copper ions and the carbons. All of the linear representations in Figs. 3 and 4 had high correlation

Table 2. Freundlich Constants for Copper Adsorption by Select Almond Shell and Commercial Carbons

Sample ID	n	K_f	r^2	p
Almond shell GACs				
AAS71	3.22	0.282	0.91	<0.01
AS70	1.73	0.057	0.97	<0.01
AAS70	3.85	0.308	0.99	<0.01
Commercial GACs				
Norit RO 3515	1.63	0.062	0.74	<0.01
Norit C	3.46	0.103	0.84	<0.01
Nuchar WV-B	2.11	0.045	0.88	<0.01

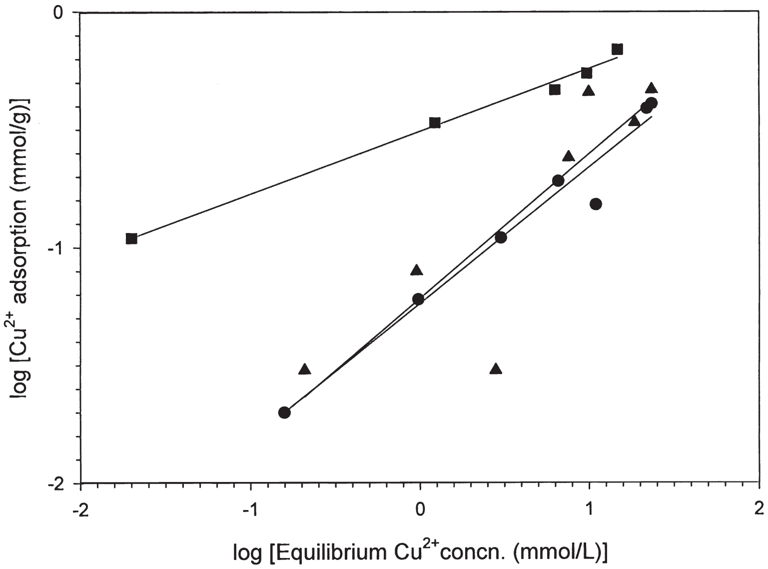

Figure 4. Freundlich plots for steam-activated, AS70 (●) $r^2 = 0.97$, and steam-activated/oxidized, AAS70 (■) $r^2 = 0.99$, almond shell-based carbons and a steam-activated, peat-based commercial carbon, Norit RO 3515 (▲) $r^2 = 0.74$.

coefficients (r^2) and the fact that $p < 0.01$ in all cases, indicates that the Freundlich model adequately represents the data.

Column Experiments

Figure 5 shows the column performance of an acid-activated almond shell carbon (AAS71) compared to two commercial acid-activated carbons (Norit C and Nuchar WV-B). The almond shell carbon achieved breakthrough much later and approached exhaustion much more slowly than the two commercial carbons. Not only does this carbon have a greater adsorption of copper ion than the comparable commercial samples, but also possesses a greater number of metal ion binding sites than the commercial carbons, as seen in its ability to reach exhaustion in a very slow manner. This is likely due to its relatively greater surface charge compared to its commercial counterparts (Table 1). For these carbons, it is unlikely that surface area plays a significant role in either influencing breakthrough values or rates of column exhaustion. For the three carbons, surface areas were similar (Table 1).

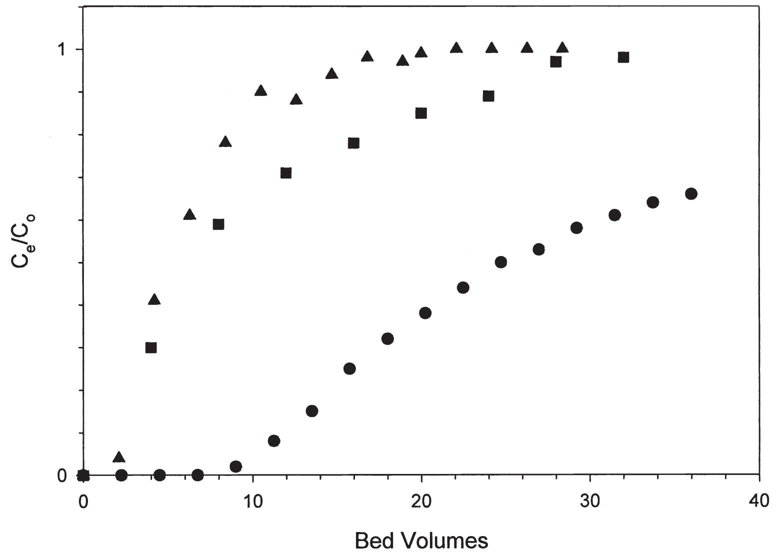

Figure 5. Column performance for phosphoric acid-activated, almond shell-based carbon, AAS71 (●), and phosphoric acid-activated, wood-based commercial carbons, Norit C (■), and Nuchar WV-B (▲). EBCT = 5 min.

Figure 6 shows the column performance of nonoxidized and oxidized, steam-activated almond shell carbons (AS70 and AAS70) compared to a steam-activated, nonoxidized commercial carbon (Norit RO 3515). Again, breakthrough was achieved later for both almond shell carbons than for the commercial carbon, in which case breakthrough occurred quickly and breakthrough volume could not be measured. Exhaustion occurred rapidly for AS70, but less rapidly for both its oxidized counterpart, AAS70 and Norit RO 3515, which were similar in their rates toward achieving exhaustion. In this case, breakthrough and rate of exhaustion were not a function of acidic surface charge. All three carbons had nearly the same surface charge and it was a net positive charge, which is not conducive to binding of positively charged metal ions. However, total titratable groups were considerably greater in the almond shell-based carbons compared to Norit RO 3515. Moreover, Norit RO 3515 had almost twice the surface area of the almond shell-based carbons. Possibly a combination of surface charge characteristics and surface area determine breakthrough and rate of exhaustion for carbons in column mode.

Table 3 gives breakthrough volumes (V_b), CURs, and EHO at two EBCT, namely 5 and 24 min. By increasing the EBCT, more metal ion can be adsorbed from the solution by allowing the column system to approach equilibrium. Since more metal ion is adsorbed, V_b and EHO should increase and CUR should decrease. Where

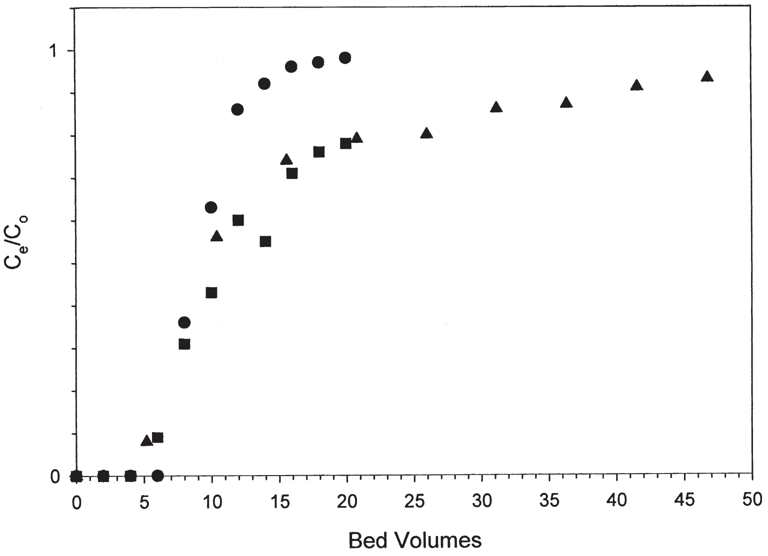

Figure 6. Column performance for steam-activated, AS70 (●), and steam-activated/oxidized, AAS70 (■), almond shell-based carbons and a steam-activated, peat-based commercial carbon, Norit RO 3515 (▲). EBCT = 5 min.

data are given, we observed this pattern for all carbons except AS70, where V_b decreased and CUR increased at the higher EBCT. Breakthrough volumes were highest and carbon usage rates were lowest for AAS71 at both EBCTs. AAS71 also had one of the highest EHOs compared to both experimental and commercial carbons.

Oxidation appeared to improve the performance of not only AAS71 but also AAS70 as well. In batch mode, AAS70 and AAS71 had comparable adsorption of copper ion, which was greater than all the other carbons evaluated. In column mode, AAS70 was also impressive, with high breakthrough volumes, at both EBCTs, low CURs, and the highest EHO of any carbon evaluated. Interestingly, these adsorption characteristics toward metal ions would not necessarily be predicted from AAS70 considering its basic surface charge and alkaline pH. However, it did have a high number of total titratable groups, especially among the almond shell-based carbons. These titratable groups are normally due to the presence of carbonyl groups and do not necessarily possess a formal charge, either positive or negative, but have a weakly negative character. They could potentially attract metal ions. Norit C and Nuchar WV-B had the highest values for titratable groups of all the carbons listed. Yet their performance in both batch and column mode was not as good as AAS71 and AAS70. Perhaps

Table 3. Select Column Parameters for Columns Packed with Almond Shell-Based Carbons or Commercial Carbons

Sample ID	EBCT (min)	V_b (mL)	CUR (g/mL)	EHO (hr)
Almond shell GACs				
AAS71	5	423	0.04	1.9
	24	1290	0.01	5.0
AS70	5	289	0.06	1.1
	24	74	0.24	4.2
AAS70	5	226	0.07	4.0
	24	380	0.04	24.0
Commercial GACs				
Norit RO 3515	5	0	—	2.1
	24	0	—	8.1
Norit C	5	0	—	0.8
	24	166	0.06	3.8
Nuchar WV-B	24	192	0.06	2.1
	5	93	0.13	0.6

EBCT = empty bed contact time; V_b = breakthrough volume; CUR = carbon usage rate; EHO = estimated hours of operation.

the types of titratable groups on the carbon surface plays a major role in carbon adsorption of metal ions as possibly does pore size distribution, neither of which were determined.

The slope of the column adsorption curves seen in Figs. 5 and 6 is related to the column's Mass Transfer Zone (MTZ). The MTZ is the zone of active adsorption by the carbon. Carbon particles above or below the MTZ (depending on the direction of column flow) are considered fully saturated with adsorbate and carbon particles below or above the MTZ are considered pristine. Depending on a number of variables, such as EBCT and the kinetics of adsorption for a particular carbon, the MTZ can either be a very small region extending a short distance from the point of effluent input (Ideal Plug Flow) or this region can extend up to a considerable distance from the input point, indicating that there is active adsorption occurring along a large portion of the column. Among the carbons examined in this study, AAS71 (Fig. 5) exhibited an extended MTZ, while AS70 and (Fig. 6) and Nuchar WV-B (Fig. 5) had much less extended MTZs.

Additionally, breakthrough and the rate at which a column approaches exhaustion are not necessarily related. For example, AS70 had a high breakthrough volume but approached exhaustion relatively quickly. AAS70 had a similar breakthrough volume but approached exhaustion more slowly than AS70. Norit RO 3515 had no measurable breakthrough volume but approached exhaustion at the same rate as AAS70. Obviously, column performance is based on a unique set of carbon adsorption kinetics and surface chemistry and is difficult to predict from adsorption behavior in batch mode.

CONCLUSION

Clearly, both in batch (equilibrium) and column (nonequilibrium) modes, AAS71 is the carbon of choice for adsorption of copper ion. It generally outperformed steam-activated and steam-activated oxidized almond shell carbons, and three different commercial samples. The most likely explanation for its good performance is its high acidic surface charge that resulted from the concurrent activation and oxidation process under which this carbon was made. Since commercial activated carbons generally do not adsorb metal ions effectively, AAS71 could fill an important niche as a carbon that can be used in metal ion remediation of water and wastewater.

DISCLAIMER

Mention of names of companies or commercial products is solely for the purpose of providing specific information and does not imply recommendation or endorsement by the U.S. Department of Agriculture over others not mentioned.

ACKNOWLEDGMENTS

This research was funded in part by a grant from the Almond Hullers and Processors Association, Turlock, CA. Thanks are extended to Lynda Wartelle, Jennifer Schissler and David Boler for their technical assistance.

REFERENCES

1. Reed, B.E.; Arunachalam, S. Use of Granular Activated Carbon Columns for Lead Removal. J. Environ. Eng. **1994**, *120* (2), 416–436.
2. Reed, B.E.; Matsumoto, M.R. Modeling Cadmium Adsorption by Activated Carbon Using the Langmuir and Freundlich Isotherm Expressions. Sep. Sci. Technol. **1993**, *28* (13 and 14), 2179–2195.
3. Corapciouglu, M.O.; Huang, C.P. The Adsorption of Heavy Metals onto Hydrous Activated Carbon. Water Res. **1987**, *21* (9), 1031–1044.
4. McKay, G.; Bino, M.J. Adsorption of Pollutants on to Activated Carbon in Fixed Beds. J. Chem. Technol. Biotechnol. **1987**, *37*, 81–93.

5. Seco, A.; Marzal, P.; Gabaldón, C.; Ferrer, J. Adsorption of Heavy Metals from Aqueous Solutions onto Activated Carbon in Single Cu and Ni Systems and in Binary Cu–Ni, Cu–Cd and Cu–Zn Systems. J. Chem. Technol. Biotechnol. **1997**, *68*, 23–30.
6. Toles, C.A.; Marshall, W.E.; Johns, M.M. Granular Activated Carbons from Nutshells for the Uptake of Metals and Organic Compounds. Carbon **1997**, *35* (9), 1407–1414.
7. Toles, C.A.; Marshall, W.E.; Johns, M.M. Phosphoric Acid Activation of Nutshells for Metals and Organic Remediation: Process Optimization. J. Chem. Technol. Biotechnol. **1998**, *72*, 255–263.
8. Toles, C.A.; Marshall, W.E.; Johns, M.M. Surface Functional Groups on Acid-Activated Nutshell Carbons. Carbon **1999**, *37*, 1207–1214.
9. Anonymous, National Statistical Service. *Agricultural Statistics 2000*; U.S. Government Printing Office: Washington, DC, 2000; V-39.
10. Toles, C.A.; Marshall, W.E.; Wartelle, L.H.; McAloon, A. Steam- or Carbon Dioxide-Activated Carbons from Almond Shells: Physical, Chemical, and Adsorptive Properties and Estimated Cost of Production. Bioresour. Technol. **2000**, *75*, 197–203.
11. Boehm, H.P. Some Aspects of the Surface Chemistry of Carbon Blacks and Other Carbons. Carbon **1994**, *32*, 759–769.
12. Toles, C.A.; Marshall, W.E.; Johns, M.M.; Wartelle, L.H.; McAloon, A. Acid-Activated Carbons from Almond Shells: Physical, Chemical, and Adsorptive Properties and Estimated Cost of Production. Bioresource. Technol. **2000**, *71*, 87–92.
13. Ferro-Garcia, M.A.; Rivera-Utrilla, J.; Rodriguez-Gordillo, J.; Bautista-Toledo, J. Adsorption of Zinc, Cadmium, and Copper on Activated Carbons Obtained from Agricultural By-products. Carbon **1988**, *26*, 363–373.
14. Reed, B.E. Wastewater Treatment: Heavy Metals. In *Environmental Analysis and Remediation*; Meyers, R.A., Ed.; Wiley: New York, 1998; 5220–5248.
15. Cheremisinoff, N.P.; Cheremisinoff, P.N. *Carbon Adsorption for Pollution Control*; Prentice-Hall: New Jersey, 1993; 216–243.
16. Clark, R.M. Water Supply. In *Standard Handbook of Environmental Engineering*; Corbitt, R.A., Ed.; McGraw Hill: New York, 1990; 5.1–5.225.
17. Rubin, A.J.; Mercer, D.L. Adsorption of Free and Complexed Metals from Solution by Activated Carbon. In *Adsorption of Inorganics at Solid–Liquid Interfaces*; Anderson, M.A., Rubin, A.J., Eds.; Ann Arbor Science: Michigan, 1981; 295–325.

Received June 2001
Revised November 2001